Theoretical and Applied Climatology
https://doi.org/10.1007/s00704-020-03404-z

ORIGINAL PAPER

Inconsistent urbanization effects on summer precipitation over the typical climate regions in central and eastern China

Fan Xiao [1,2,3] · Bin Zhu [1,2,3] · Tong Zhu [4]

Received: 24 February 2020 / Accepted: 21 September 2020

Abstract
Using a 30-year data (1983–2012) from 428 stations, we study summer precipitation differences between urban and rural areas in 5 Chinese climate regions: the Pearl River Delta (PRD), the Middle and Upper reaches of the Yangtze River (MUYR), the Yangtze River Delta (YRD), the North China Plain (NCP), and Northeast China (NEC). By analyzing heavy rain (HR) (24-h precipitation ≥ 100 mm) and light rain (LR) (0.1 mm ≤ 24 h precipitation ≤ 25 mm), we find that urbanization has had inconsistent effects on precipitation. Higher HR occurs over urban areas of the PRD and YRD than rural areas, and lower HR occurs over urban areas of the MUYR, NCP and NEC than rural areas. The urban LR is less than the rural LR in all climate regions. The correlation between precipitation and the convective available potential energy (CAPE) or humidity explains the regional differences in urbanization effects on HR. HR is greatly affected by the CAPE in the PRD and YRD, where the CAPE is high (> 600 J/kg at 14:00 LT), water vapor is abundant (> 45 kg/m^2 at 14:00 LT), and the urban heat island increases the urban HR. However, HR is greatly affected by humidity in the MUYR, NCP, and NEC, where the CAPE and water vapor are less (≤ 500 J/kg and ≤ 40 kg/m^2 at 14:00 LT) and the urban HR is mainly suppressed by the urban dry island. Our results indicate that urbanization promotes HR in wet climates but suppresses HR in dry climates during summer in central and eastern China.

Keywords Different climate zones · Precipitation of different intensities · Inconsistent urbanization effects on precipitation · Physical mechanism

1 Introduction

Over the past 30 years, China has experienced rapid urbanization. A series of environmental variations, such as underlying surface replacement, population surges, and pollution emissions, have changed the physical and chemical properties of the urban atmosphere, and these variations have complex impacts on meteorological factors, such as temperature, humidity, and precipitation (Yang et al. 2011; Hao et al. 2013; Song et al. 2014; Han et al. 2014; Li et al. 2016). Researchers have suggested that the impacts of urbanization on precipitation mainly originated from three factors (Baik et al. 2001; Rozoff et al. 2003; Baik et al. 2007): urban heat island (UHI) effects (Olfe and Lee 1971; Changnon 1979; Baik 1992; Bornstein and Lin 2000; Kaufmann et al. 2007; Han and Baik 2008; Lin et al. 2011; Li et al. 2011a; Wang et al. 2015; Liang and Ding 2017), underlying surface changes (such as urban dry island (UDI) effects caused by decreases of low-layer atmospheric humidity) (Zhang et al. 2009; Kishtawal et al. 2010; Miao et al. 2011; Souma et al. 2013; Wu and Tang 2015; Zhou et al. 2015), and aerosol emissions (Houze 1993; Pruppacher and Klett 1997; Rosenfeld 2000; Zhang et al. 2009; Li et al. 2011b; Guo et al. 2014; Li et al. 2019).

The impacts of urbanization on precipitation vary regionally as revealed by previous studies; thus, it is often difficult to determine the dominant factors of urbanization effects due to

✉ Bin Zhu
binzhu@nuist.edu.cn

[1] Collaborative Innovation Centre on Forecast and Evaluation of Meteorological Disasters, Nanjing University of Information Science & Technology, Nanjing, China

[2] Key Laboratory of Meteorological Disaster, Ministry of Education (KLME), Nanjing University of Information Science & Technology, Nanjing, China

[3] Special Test Field of National Integrated Meteorological Observation, Nanjing University of Information Science & Technology, Nanjing, China

[4] IM System Group, Inc. @NOAA/NESDIS/STAR, College Park, MD, USA

Published online: 06 October 2020

the joint effects of local geography and climatic background (Han et al. 2014; Li et al. 2016). Some researchers agreed that urbanization enhances precipitation (Changnon 1979; Baik et al. 2001; Mote et al. 2007; Zhang et al. 2010; Lin et al. 2011; Li et al. 2011a; Wang et al. 2015; Liang and Ding 2017); some suggested that urbanization suppresses precipitation (Kaufmann et al. 2007; Zhang et al. 2009; Wu and Tang 2015; Zhou et al. 2015), while others suggested that urbanization showed no obvious effects on precipitation (Tayan and Toros 1997). Generally, the UHI is caused directly by urbanization and referring to the phenomenon that the temperature of city is higher than that of the surrounding suburban or rural areas (Oke 1973), and it affects precipitation by changing the urban thermodynamic field (Han et al. 2014). The UHI reduces the stability of the atmospheric layer by forming heat island circulation, which is conducive to trigger convection and form convective precipitation, and then affects the distribution of precipitation over cities and their downstream areas (Olfe and Lee 1971; Baik 1992; Han and Baik 2008). As early as the 1970s, METROMEX confirmed the urbanization effect of increasing rainfalls through 5-year intensive observations and found that precipitation within 50 to 75 km of the St. Louis city core and its downwind areas increased by 25% compared with the background areas (Changnon 1979). Lin (2011) suggested that the UHI has strengthened precipitation in Taipei and its downwind areas and affected the time and location of rainfall systems. Similarly, some studies in China agreed that urbanization has led to increases of convective precipitation over many places, such as the urban agglomerations of the Pearl River Delta (PRD) (Li et al. 2011a), the city core of Shanghai (Liang and Ding 2017), and the city lower reaches of Beijing (Wang et al. 2015).

However, the inhibitory urbanization effects on precipitation have been found in some studies (Kaufmann et al. 2007; Zhang et al. 2009; Wu and Tang 2015; Zhou et al. 2015). The UHI increases the temperature of the urban boundary layer and lifts the cloud base height, which lengthens the raindrop falling path, resulting in the evaporation of light raindrops. In addition, the decreasing atmospheric water vapor supplied by urban surfaces is also a possible reason for the decrease of urban light rain (Kaufmann et al. 2007). Urban surfaces, which are mostly replaced by artificial surfaces (such as concrete), have weaker water permeability, higher thermal conductivity and lower heat capacity than natural surfaces (Shem and Shepherd 2009). So urban surfaces often cause UDI effects, which suppress urban precipitation (Zhang et al. 2009). The urbanization processes in the Yangtze River Delta (YRD) (Wu and Tang 2015), the PRD, and the Beijing-Tianjin-Hebei (Zhou et al. 2015) expand the surface impervious areas, leading to reductions in surface evaporation and local atmospheric moisture, thereby decreasing summer precipitation.

A large amount of gaseous pollutants and aerosols are emitted during urban production and life, and some of them act as cloud condensation nuclei (CCNs), which participate in microphysical processes and cloud precipitation processes or affect precipitation through radiation effects of scattering and absorption (Han et al. 2014). The aerosol effect on precipitation is highly uncertain and related to aerosol size, quantity, chemical composition, cloud type, precipitation type, climatic and geographical conditions, and other factors (Houze 1993; Pruppacher and Klett 1997; Li et al. 2019). The long-term simulation results of Zhang et al. (2010) showed that aerosols in the YRD increase the water vapor mixing ratio of the urban boundary layer and cause significant enhancement of urban precipitation.

Under the combined influences of the above factors (such as the UHI, aerosol, and underlying surface), the effects of urbanization on precipitation become uncertain. Some scholars believed that whether urbanization increases (Mote et al. 2007), triggers (Baik et al. 2001), or decreases (Zhang et al. 2009) precipitation depends on the relative importance of various factors (Baik et al. 2001; Han et al. 2014; Wang et al. 2015; Li et al. 2016) related to the scale of the city and its surrounding geographic features. For example, in the early stage of urbanization, the UHI plays a dominant role in the enhancement of precipitation in a city. As the water supply of the underlying surface continues to decrease, the inhibition of urbanization on precipitation will gradually increase, which will offset some of the UHI enhancement to precipitation (Wang et al. 2015). Other scholars have proposed that urbanization increases the surface roughness, which reduces the surface wind speed and results in the convergence of near-surface wind fields (Baik et al. 2001). When considering the aerosol effects on precipitation, on the one hand, it increases the retention time of cloud droplets in air and promotes the condensation growth of cloud droplets, thus enhancing precipitation, while on the other hand, its absorption effect of radiation can warm the atmosphere and cool the surface, which makes the atmospheric stratification more stable, resulting in an opposite effect on the precipitation as compared with the UHI (Han et al. 2014).

The above studies have shown urbanization impacts on local precipitation, and these studies mostly focused on one single city or city cluster over one region (Shastri et al. 2015), with few comprehensive studies investigating different intensities of precipitation over different climate regions. Due to regional variations in the main contributors that affect precipitation, the dominant factors in different climate regions are still poorly understood. However, the classification of urban and rural sites is a significant cornerstone when researching urbanization impacts on precipitation. Formerly, station classification was based on single data types, such as population (Hua et al. 2008), land type (Yang et al. 2013), gross domestic product (GDP) (Guo et al. 2016), night light (Yan et al. 2019), and impervious surface area (ISA) (He et al. 2017). Considering that our research areas are relatively large,

including central and eastern China, we combine data observed by satellite, such as night light, population, ISA and GDP, and other aspects to define urban stations and rural stations. Based on the differences between urban and rural meteorological and climatic factors (such as the UHI, UDI, convective instability energy, water vapor content, and dew-point deficit), we explore the inconsistent urbanization impacts on precipitation between urban and rural areas over different climate regions. This analysis can provide a deeper understanding of the responses of different intensities of summer rainfall to urbanization and scientific bases for assessments of local urbanization impacts on precipitation in various climates.

2 Data and methods

2.1 Data

The main dataset employed in this article is the daily observation dataset after quality control provided by the National Meteorological Information Center of China, including 2-m atmospheric temperature (TEM), relative humidity (RH), visibility (VIS), and daily precipitation (P). The time span of these data includes summers from 1983 to 2012 (June, July and August). The rainfall data were recorded every hour, while other data were recorded four times per day (02:00, 08:00, 14:00, and 20:00 LT). The data source is http://data.cma.cn/en.

The China gridded population dataset in km (Population Grid China) provides population data for 2010. The data spatial resolution is 1 km, and it can be obtained from the Global Change Science Research Data Publishing System (http://www.geodoi.ac.cn).

The defense meteorological satellite program/operational line-scan system (DMSP/OLS) provides ISA data for 2000, GDP data for 2006, and night light data for 2010. The spatial resolution is 30 arc sec (approximately 1 km). The ISA data range from 0 to 100%, and the night light data range from 0 to 63. The data source is https://www.ngdc.noaa.gov/eog/dmsp.html.

The data on the convective available potential energy (CAPE), 2 m dew-point deficit, and total column water vapor are derived from the European Center for Medium-Range Weather Forecasts (ECMWF/ERA-Interim), with a spatial resolution of 0.125° and time period from 1983 to 2012 (only including June, July, and August). The data source is https://apps.ecmwf.int/datasets/data/interim-full-daily/levtype=sfc/.

2.2 Study region

The research regions in this paper are mainly distributed in central and eastern China, and five different climatic regions are selected as representative regions. As shown in Fig. 1, from south to north, the five different climatic regions are as follows: the PRD, belonging to the south subtropical marine zone; the middle and upper reaches of the Yangtze River (MUYR), belonging to the subtropical zone of the continent; the YRD, belonging to the northern subtropical marine zone; the North China Plain (NCP), belonging to the warm temperate zone; and Northeast China (NEC), belonging to the moderate temperate zone. The PRD is one of the three major urban agglomerations with the largest population and the strongest economic strength in south China. The Yangtze River is the largest river in Asia, and the MUYR is close to the Tibet plateau, and the local topography is complex, which includes the Sichuan Basin and mountains, thus forming a complex local climate. Moreover, this area has the largest population in western China, with its gross national product accounting for 36% of the total for China. Its downstream area (YRD) is the alluvial plain before the Yangtze River enters the sea. The YRD city cluster is one of the six internationally recognized world-class city clusters and the largest economic zone in China. The NCP is the largest and most dynamic region in the northern part of China, and it is the location of the national capital city. The NEC region has vast mountains and rich forests, and its total amount of forest storage accounts for about one-third of the total in China. Each area has their own unique climate type and urbanization process.

According to Fig. 1a, precipitation and CAPE are distinctive in five climatic zones and generally decrease from south to north, and they are larger in the PRD and YRD than in the MUYR, NCP, and NEC, with the CAPE of NEC particularly low.

2.3 Station classification

Considering that one single variable cannot reflect the degree of urbanization well, here, we use a combined dataset of four different types to divide urban and rural sites. He et al. (2017) found that different ISA values show different impacts on the ecological environment. In their study, the ISA within [1%, 10%) means the ecology suffered a slight urbanization impact; the ISA within [10%, 25%) means the urbanization impact became obvious; the ISA exceeded 25% means the ecological environment began to degrade. Therefore, grids where the meteorological station is located as the center grid are selected. If the ISA is at least in one grid among the center grid and its surrounding eight grids exceeds 10%, then this station is regarded as a city station, and if at least one grid of the ISA exceeds 25%, then it is regarded as a large city station. Based on the ISA, we found that 33% of the stations (2420 in total) fit the city station condition and 21% of the city stations fit the large city station condition. Because the ISA can only represent differences of underlying surface between urban and rural areas, which may lead to inaccurate station type

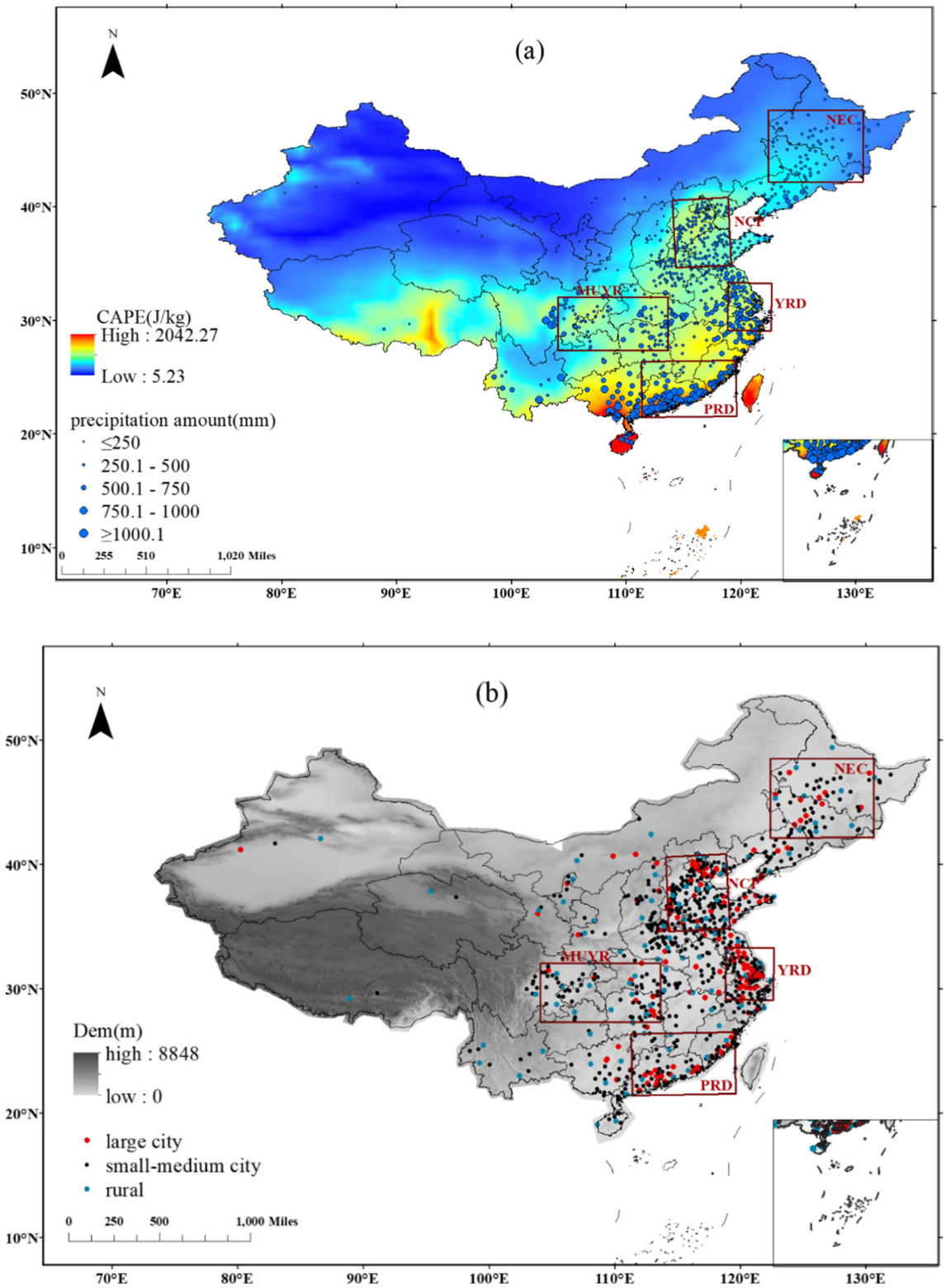

Fig. 1 **a** Distributions of summer average precipitation and CAPE; **b** elevation distributions and station locations and types. Blue circles indicate precipitation, colored blocks indicate CAPE, red dots represent large city stations, black dots represent small-medium city stations, blue dots represent rural stations, and red squares represent the five different climate regions from south to north: PRD (77 stations), MUYR (64 stations), YRD (80 stations), NCP (149 stations), and NEC (58 stations)

identifications, we added night light, GDP, and population data to obtain a more accurate judgment of urban and rural stations. Considering that the selection region range of night light data for one station cannot be too large or too small (Yan et al. 2019), we calculate the average night lights, GDP, and population in the square with a side length of 7 km (7 × 7 grids) centered on each station. To weaken the influence of altitude in this study, the altitude difference of selected stations with the median altitude of each province is controlled within 200 m. If a station meets the altitude requirements and its sequence is in the top 33% of total stations determined by two of the four types of data (population, night light, ISA, and GDP), it is classified as a city station. Similarly, if its sequence is in the top 21% of city stations, it is classified as a large city station. For city stations, except large city stations, the rest are small-medium city stations. Among the nonurban stations that meet the altitude requirements, rural stations are selected based on the "Technical Requirements for the Selection of National Reference Climate Station Sites" (Guo 2014) and the characteristics of persistent and stable location during the study period.

In this study, the five regions we selected are more urbanized and have 428 stations in total, including 104 large city stations, 283 small-medium city stations, and 41 rural stations. The numbers of sites per station type in the five climate regions are listed in parentheses as follows: PRD (22, 47, 8), MUYR (8, 46, 10), YRD (34, 42, 4), NCP (31, 107, 11), and NEC (9, 41, 8). The distributions and classifications of stations are shown in Fig. 1b.

2.4 Precipitation classification

According to the national 24-h precipitation-level standard of China (GB/T28592-2012), precipitation is divided into six levels (Table 1). A single precipitation event has an amount of more than 0.1 mm and a duration of more than 1 h. The 24-h rainfall amount (y in mm) of a single precipitation event is converted according to the duration (tx in h) of the actual precipitation amount (x in mm) from Eq. (1), and then the precipitation is classified based on y (Table 1):

Table 1 Precipitation level division

Range	Rank	Name
0.1 ≤ y ≤ 9.9 mm	1	LR: light rain
10.0 ≤ y ≤ 24.9 mm	2	
25 ≤ y ≤ 49.9 mm	3	
50.0 ≤ y ≤ 99.9 mm	4	
100 ≤ y ≤ 249.9 mm	5	HR: heavy rain
250 mm < y	6	

$$\frac{x}{tx} = \frac{y}{24} \rightarrow x \times \frac{24}{tx} = y \tag{1}$$

2.5 Other data processing methods

The differences calculation method between urban and rural physical quantity (precipitation, temperature, RH) involves subtracting the value of rural stations from that of urban stations. To avoid the bias caused by one single rural station, we did not use the method of calculating the differences between the nearest urban and rural stations. Here, we select the average value of rural stations with altitude differences of less than 100 m from the target urban station in the same region as the rural value corresponding to the target urban stations in each region. This method also minimizes the impact of altitude on physical quantity differences between urban and rural stations.

3 Results and discussion

3.1 Differences in precipitation between urban and rural areas

3.1.1 Long-term temporal variations

Figure 2 shows the annual variations in six different levels of precipitation (based on GB/T28592-2012) during the summers of 1983–2012 over urban and rural stations. The durations, counts, and amounts of precipitation differences between urban and rural stations exhibit similar results. Levels 1 to 3 of precipitation over rural stations are significantly higher than those over urban stations, and the precipitation differences between large cities and small-medium cities are small. The precipitation differences at level 4 between urban and rural stations are small, and levels 5 to 6 of precipitation over urban stations are higher than those over rural stations. Because the differences between urban and rural stations in three precipitation characteristics in Fig. 2 are similar, subsequent studies only selected the precipitation amounts for analysis. Figure 3 shows the 30-year mean precipitation differences among the three station types and is consistent with the results shown in Fig. 2, among which the amounts of urban-rural precipitation differences are more obvious. Urbanization effects are inconsistent for different intensities of precipitation, and they inhibit weak precipitation (levels 1–3) and weakly promote strong precipitation (levels 4–6). However, as the intensity of precipitation increased in levels 5 and 6, the enhancement effects of urbanization on precipitation became obvious, which can be seen from the significant

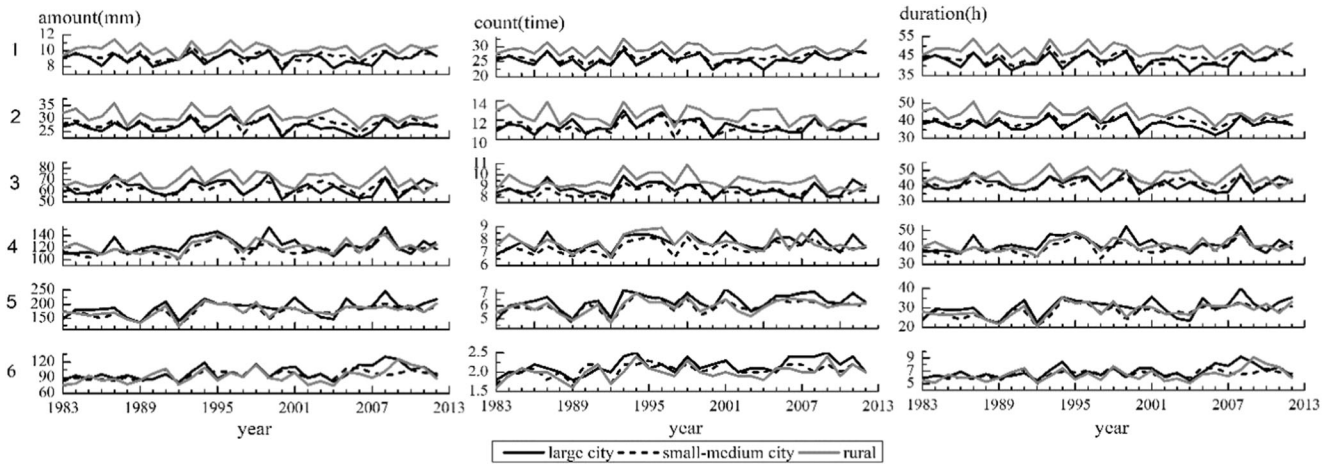

Fig. 2 Annual changes in precipitation counts, amounts, and durations of different levels over urban and rural stations. Numbers 1 to 6 represent six diverse levels of precipitation (Table 1); black solid lines represent large city stations, black dotted lines represent small-medium city stations, and gray solid lines represent rural stations

differences represented by *P* values in Fig. 3 (one-way analysis of variance (ANOVA), with a smaller *P* value indicating more significant differences). To more clearly study the differences in various intensities of precipitation, levels 1 to 2 of precipitation are collectively referred to as LR (light rain), while levels 5 to 6 of precipitation are collectively referred to as HR (heavy rain). In particular, the precipitation in transition states (levels 3–4) has been excluded. The urban-rural differences in LR amounts and durations have passed the 95% significance test, although the urban-rural differences in HR are nonsignificant. Only when the precipitation intensity reaches the highest level and the urban size is large are the HR differences between urban and rural significant.

3.2 Diurnal variations

Figure 4 shows the diurnal variation characteristics of the 30-year summer average precipitation amounts. The diurnal distributions of precipitation vary for different intensities. LR is the "double peak" type, and HR is the "single peak" type. The diurnal distributions of urban and rural stations are basically identical, although the afternoon peak of urban HR is slightly earlier than that of rural, which may be related to that ability of the UHI to trigger precipitation formation. Previous observations and numerical simulation studies demonstrated that UHIs induce convergence zones and then initiate storms (Bornstein and Lin 2000; Baik et al. 2001; Rozoff et al. 2003).

Urbanization effects do not alter the diurnal variations in precipitation. Thus, because temperature and humidity present

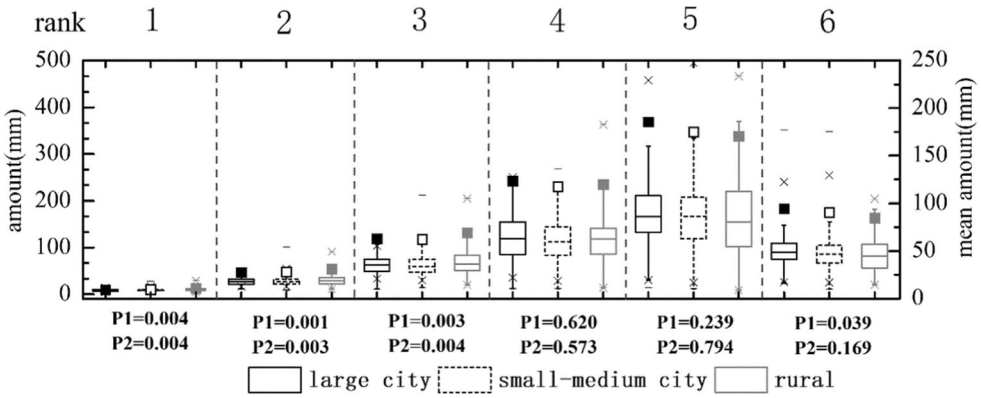

Fig. 3 Annual average precipitation amounts of different levels at urban and rural stations. Numbers 1–6 represent six diverse levels of precipitation (Table 1). The left vertical axis is the precipitation value corresponding to the box plot, and the right vertical axis is the average precipitation value corresponding to the point plot. Please note that the 2 vertical axes are in different ranges. The black solid box represents large cities, the black dotted box represents small-medium cities, the gray solid box represents rural stations, the square points are mean values, the black solid square points are mean values of large cities, the black dotted square points are mean values of small-medium cities, and the gray solid square points are mean values of rural. The upper and lower frame boundaries are the upper and lower quartiles, the upper and lower horizontal lines are the upper and lower limits, and × is the abnormal value. P1 is the significance of the difference between large cities and rural stations, and P2 is the significance of the difference between small-medium cities and rural stations

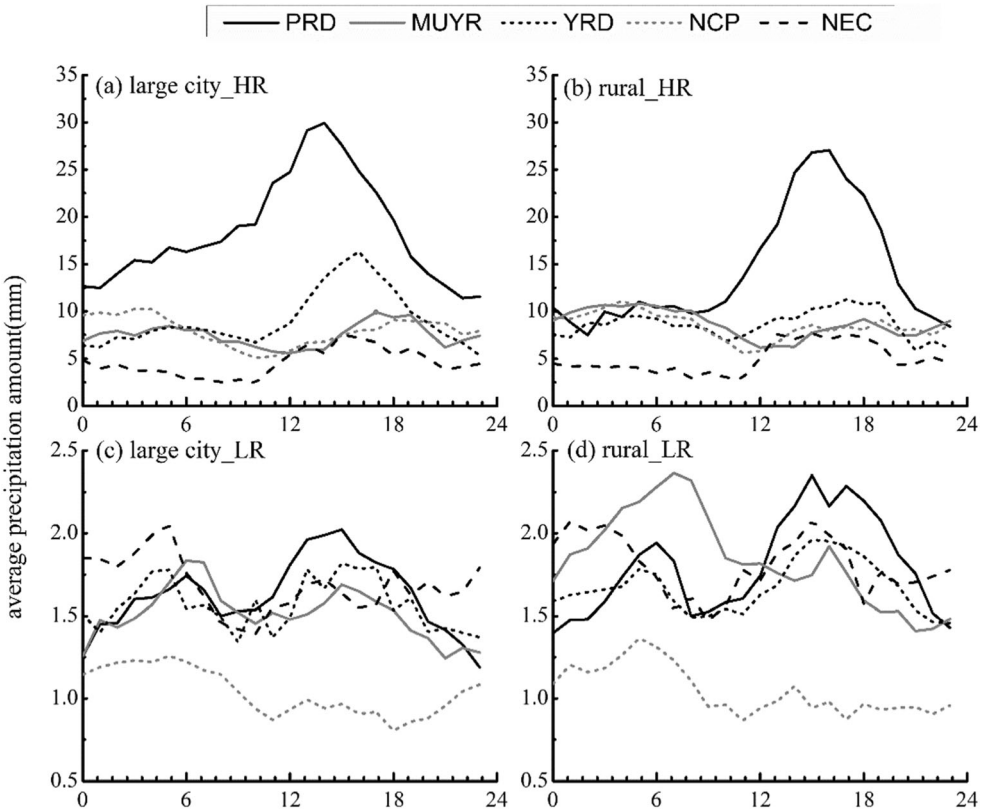

Fig. 4 Diurnal variations in annual precipitation amounts per station in summer. **a** HR over large city stations, **b** HR over rural stations, **c** LR over large city stations, and **d** LR over rural stations. The horizontal axis represents the local time, and the vertical axis indicates the number of precipitation events

diurnal variations, precipitation may be connected to the local temperature and humidity environment; therefore, the existence of the UHIs and UDIs may cause precipitation differences between urban and rural areas.

Some previous studies found that urbanization would delay urban HR (Rosenfeld 1999; Rosenfeld et al. 2008). Rosenfeld (1999) indicated that under the condition of insufficient water vapor, urbanization may inhibit the precipitation and delay the occurrence time of urban precipitation. In areas with sufficient water vapor, Ntelekos et al. (2009) found that precipitation will increase with increases of aerosol. To investigate the delay effect, we analyzed the time series of the peak of HR starting time over the PRD and YRD regions during the 30 years. However, only a small delay signal was observed (not shown), and the fitted trend did not pass the 90% significance test. The urban aerosol effect on precipitation is complex, and urban aerosol cannot only participate in the precipitation process as a CCN but also affect the precipitation process through radiation and other effects. In this study, an analysis on the effect of aerosols was not performed. Additional studies are needed to investigate the combined impacts of the UHI and increased urban aerosols on precipitation under urbanization.

3.2.1 Regional disparities

Figure 5 shows the LR and HR differences between urban and rural areas over five typical climate regions. It is found that the precipitation differences between urban and rural areas vary regionally. Especially for HR, the precipitation differences over the urban stations of the PRD and YRD are higher than those over rural stations, while those over the urban stations of the MUYR, NCP, and NEC are lower than those over rural stations. The results of urban-rural precipitation differences in the PRD, YRD, and NCP also revealed by previous studies (Li et al. 2011a; Jiang et al. 2016; Wang et al. 2015; Liang and Ding 2017), while less research has been performed in the MUYD and NEC. Although the city scales and development levels of the PRD, YRD, and NCP are close to each other, the NCP shows different urbanization effects of HR. The urbanization impacts on HR may be related to the regional climate background. Shastri et al. (2015) found that urbanization impacts on heavy precipitation have regional characteristics in India; therefore, some of the driving factors affecting HR in different climate regions may differ, which would lead to regional disparities in HR differences between urban and rural areas. However, the LR distributions in Fig. 5 are higher over rural areas than urban areas in all regions, indicating that the urbanization impacts on LR are dominated by inhibitory effects, which is consistent with previous studies showing that stratiform cloud precipitation is primarily inhibited by UDI (Kaufmann et al. 2007; Kishtawal et al. 2010).

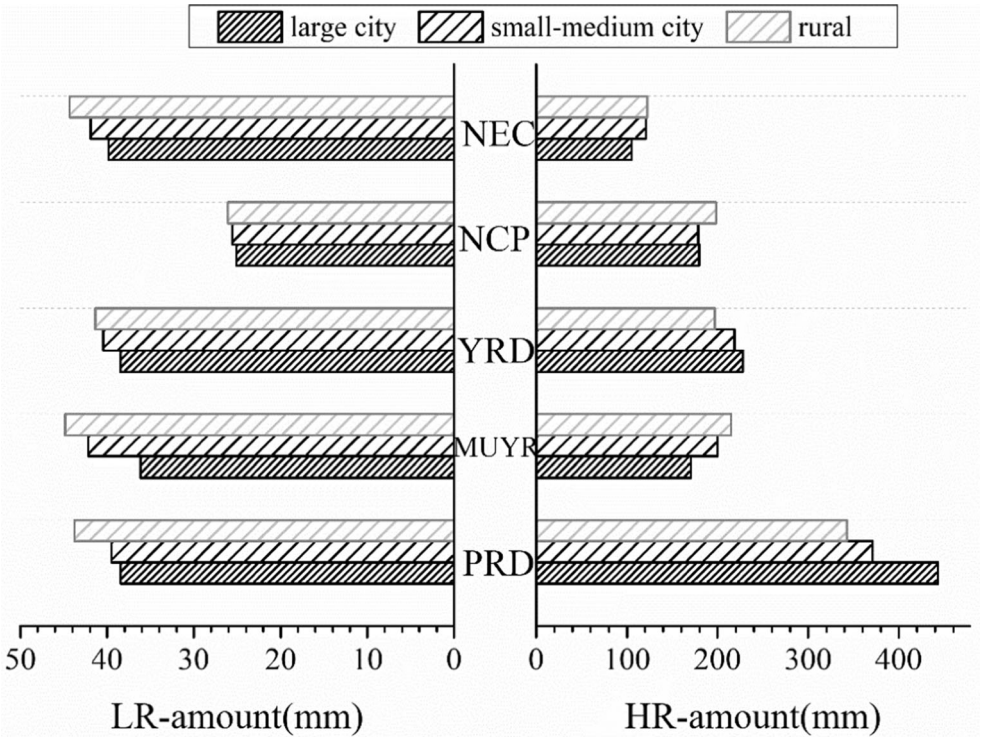

Fig. 5 Average annual summer rainfall of urban and rural stations in five climate regions. LR is shown on the left, and HR is shown on the right

3.3 Reasons for urban-rural precipitation differences

3.3.1 Relative dependence of precipitation on convective unstable energy and humidity

According to the analysis in the prior section (3.2), afternoon (12:00–18:00) may be the period when the UHI has the strongest influence on convective precipitation. During this period, both the height and turbulence intensity of the boundary layer are the largest, and the atmospheric state is unstable. Therefore, it is beneficial to trigger or strengthen the development of convective motion (Baik et al. 2007). Because the highest temperature and lowest RH occur in the daytime (picture omitted), convective precipitation may be simultaneously promoted by high temperature and suppressed by low humidity. Studying precipitation during this period may provide insights on the dominant factors affecting convective precipitation. Considering that the LR peak mainly occurs at night (00:00–06:00) in all regions (Fig. 4c, d), Fig. 6c, d extracts LR of nighttime period (00:00–6:00) (although the LR peak also occurs in the afternoon (12:00–18:00), it is not obvious in this period in the MUYR and NCP). In this study, we used the long-term observation precipitation data which limited us to specifically separate convective cloud precipitation and stratiform cloud precipitation. According to the high intensity characteristic of convective cloud precipitation and the short time, and long duration characteristics of stratiform cloud precipitation, it is believed that LR mainly reflects the characteristics of stratiform cloud precipitation, while HR mainly reflects the characteristics of convective cloud precipitation.

The CAPE is mainly used to characterize the unstable energy of the atmosphere. Convective precipitation may increase with the increase of atmospheric convective instability (Lepore et al. 2015). The CAPE and water vapor content of the whole layer in the PRD and YRD are higher than that in the MUYR, NCP, and NEC, while the dew-point deficit in the PRD and YRD is smaller than that in the MUYR, NCP, and NEC. This finding indicates that the PRD and YRD have more convective energy and are more moist within the low layers (CAPE > 600 J/kg at 14:00 LT and water vapor content > 45 kg/m2 at 14:00 LT in the PRD and YRD; CAPE ≤ 500 J/kg and water vapor content ≤ 40 kg/m2 at 14:00 LT in the MUYR, NCP, and NEC). The dew-point deficit and the water vapor content of whole layer can be used to characterize the humidity of the atmosphere. A small dew-point deficit and large water vapor content are indicative of a moist atmosphere and favorable for precipitation. Figure 6a, b, and d show that precipitation is positively correlated with the water vapor content and CAPE of entire layers, while regions of a larger CAPE tend to have higher humidity. Dong et al. (2019) found that the impacts of the CAPE and atmospheric precipitable water on precipitation showed the opposite correlations in various regions. Their results showed that the efficiency of water vapor conversion to precipitation is higher in dry climates over northern China than in wet climates over southern China, which means that in the dry

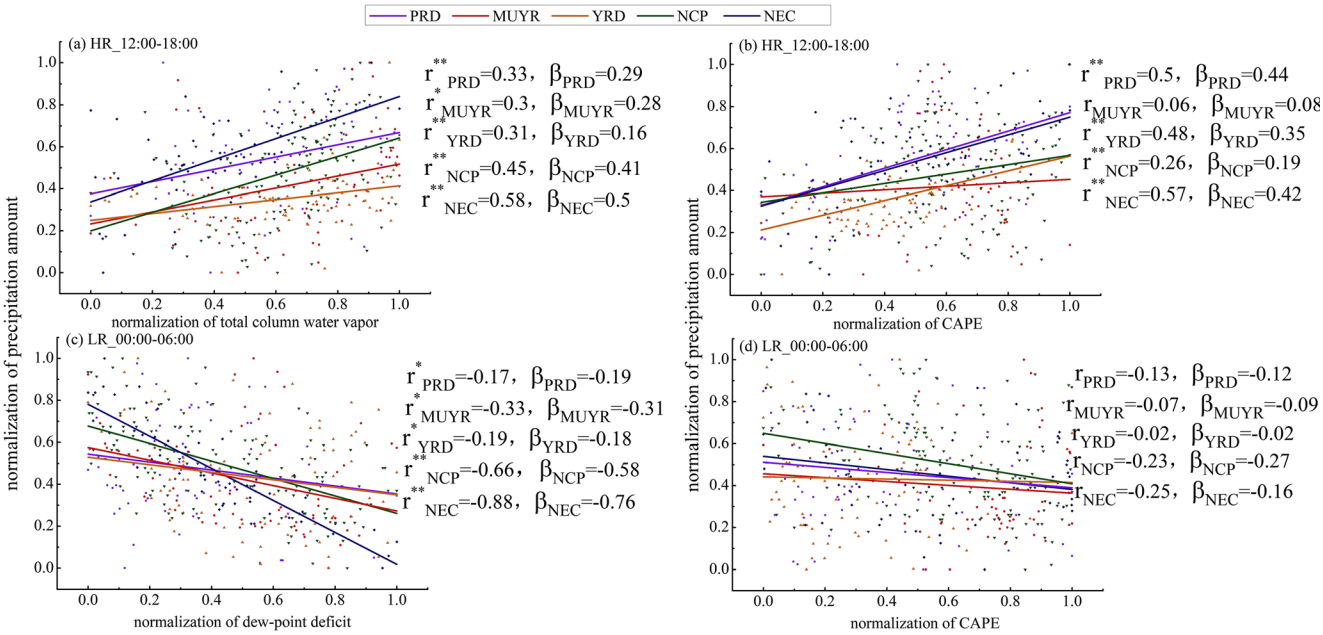

Fig. 6 Relationships among the CAPE, water vapor content of the whole layer, 2 m dew-point deficit, and precipitation in different regions during the summers from 1983 to 2012. **a** Relationship between HR from 12:00 to 18:00 and water vapor content at 14:00; **b** relationship between HR from 12:00 to 18:00 and CAPE at 14:00; **c** relationship between LR from 00:00 to 06:00 and 2 m dew-point deficit at 02:00; and **d** relationship between LR from 00:00 to 06:00 and CAPE at 02:00. *r* is the correlation coefficient, *a* is the slope, and each physical quantity has been normalized. ** indicates that the value passed the 99% significance test, and * indicates that the value passed the 98% significance test

climates of northern China, precipitation is mainly related to the water vapor content. In contrast, the efficiency of CAPE conversion into the airflow rising speed of atmospheric vertical motion is higher in humid climates over southern China, which means that in humid climates of southern China, precipitation is mainly related to the CAPE.

The relative dependence of precipitation on the CAPE and humidity can be summarized via the following regression equation:

$$y = \beta x + constant \tag{2}$$

where y is the HR or LR; x is the CAPE, water vapor content of the whole layer, or 2 m dew-point deficit; and β represents the efficiency of x being converted to y. In Fig. 6, r represents the degree of fitting, and r values closer to 1 indicate a higher fitting correlation. To directly compare the value of β, all physical quantities in Fig. 6 have been normalized.

In the PRD and YRD, the conversion efficiency of the CAPE to HR (β_{PRD} = 0.44 and β_{YRD} = 0.35 in Fig. 6b) is higher than the conversion efficiency of water vapor content to HR (β_{PRD} = 0.29 and β_{YRD} = 0.16 in Fig. 6a). In contrast, in the MUYR, NCP, and NEC, the efficiency of converting water vapor content into HR (β_{MUYR} = 0.28, β_{NCP} = 0.41, and β_{NEC} = 0.5 in Fig. 6a) is higher than the efficiency of converting CAPE into HR (β_{MUYR} = 0.08, β_{NCP} = 0.19, and β_{NEC} = 0.42 in Fig. 6). A statistical analysis indicated that the HR in the PRD and YRD may be mainly affected by the conversion of the CAPE into the airflow rising speed of atmospheric vertical motion, which means that the HR differences between urban and rural areas may be greatly affected by the UHI, and causes more urban HR. Nevertheless, the HR in the MUYR, NCP, and NEC may be more affected by the efficiency of converting water vapor into cloud droplets and raindrops, which signifies that the HR differences between urban and rural areas may be greatly affected by UDI. Urban evaporation decreases and temperature increases, which results in lower humidity and HR over urban areas than rural areas. As the HR of the MUYR, NCP, and NEC is mainly affected by the water vapor content, HR may be greatly inhibited by the UDI in these regions. However, the HR of the PRD and YRD is mainly affected by the CAPE, where the UHI may greatly promote urban HR. The above results are also consistent with the positive HR differences between urban and rural areas in the PRD and YRD and the negative HR differences in the MUYR, NCP, and NEC (Fig. 5). Except for the MUYR, the HR in all regions passed the 99% significance test. In the MUYR, the relationship between HR and water vapor content passed the 98% significance test (Fig. 6b, d). Considering the high altitude of the Sichuan-Chongqing region (close to the MUYR), which has an undulating terrain and is close to the Qinghai-Tibet Plateau, HR is affected by other factors, which may weaken the influence of the CAPE on HR (Liang et al. 2013). A previous study showed that based on the unique topography, summer rainfalls over the MUYR (especially

Sichuan) are often triggered by sub-synoptic scale cyclones near the southeastern TP (Tibet Plateau) (so-called the Southwest Vortex by Chinese meteorologists), troughs in the westerlies, shear lines, and fronts over East Asia (Jiao et al. 2005). Other researchers proposed that the MUYR rainfalls may have directly originated from the TP (Jiang and Fan 2002). Some scholars think (Mote et al. 2007) that only when other weather systems are relatively weak, the heat island circulation plays a dominant role in local weather or climate by changing the boundary layer structure, which then leads to an obvious impact on precipitation. Therefore, in the MUYR, the UHI effect on precipitation may be obscured by the influence of other weather systems, resulting in a very small correlation between precipitation and the CAPE (r values in Fig. 6b, d). The results of Guo and Li (2009) also showed that the summer precipitation of the MUYR had a significant positive correlation with the precipitable water vapor, although the correlation between precipitation and local temperature was not obvious.

The efficiency of converting water vapor content into LR in all regions ($\beta_{PRD} = -0.19$, $\beta_{MUYR} = -0.31$, $\beta_{YRD} = -0.18$, $\beta_{NCP} = -0.58$, $\beta_{NEC} = -0.76$) is higher than the conversion efficiency of CAPE ($\beta_{PRD} = -0.12$, $\beta_{MUYR} = -0.09$, $\beta_{YRD} = -0.02$, $\beta_{NCP} = -0.27$, $\beta_{NEC} = -0.16$) (Fig. 6d), indicating that LR is mainly affected by humidity and inhibited by the UDI, which is consistent with the results that less LR occurs over urban areas than rural areas (Fig. 5). The correlation of LR and dew-point deficit in all regions passed the 98% significance test, although the correlation between LR and the CAPE in most regions was nonsignificant, indicating that LR is mainly related to regional humidity and less affected by convective unstable energy.

3.3.2 Relative dependence of urban-rural precipitation differences on the UHI and UDI

The previous sections indicated that the urbanization effects on HR are inconsistent over different climate regions. Some regions are mainly affected by the CAPE (related to the UHI), while others are greatly affected by humidity. Cities generally show higher temperature and lower humidity than rural areas, which means that $\triangle T > 0$ and $\triangle RH < 0$. $\triangle T$ and $\triangle RH$ usually have opposite effects on urban HR.

The relative dependence of urban-rural precipitation differences on the UHI and UDI can be summarized with a regression equation:

$$\triangle y = \alpha \triangle z + constant \tag{3}$$

where $\triangle y$ is the HR or LR difference between urban and rural areas, $\triangle z$ is the $\triangle T$ (UHI intensity) or $\triangle RH$ (UDI intensity), and α represents the efficiency of $\triangle z$ to $\triangle y$. To directly compare the value of α, all physical quantities in Eq. (Baik et al. 2007) have been normalized.

The HR is more sensitive to CAPE in the PRD and YRD, where the water vapor condition is sufficient, and the UHI has greater effects on HR differences between urban and rural areas (α_{PRD} in Fig. 7a, c > α_{PRD} in Fig. 7b, d, respectively). Hence, in polluted cities, strong atmospheric upward motion can transport aerosols to the upper air and then increase the numbers of CCNs, which helps enhance the conversion efficiency of cloud droplets to raindrops and precipitation when water vapor is sufficient (Choi et al. 2008). Therefore, the PRD and YRD appear as "urban rain islands" for HR (Fig. 5). It is worth mentioning that the PRD has higher precipitation than other regions (Fig. 1a), which shows a negative difference in temperature and positive difference in humidity between urban and rural areas in the afternoon (Fig. 7c, d). These differences may be related to the cooling and humidification caused by precipitation itself and the moisture brought by sea breezes from coastal maritime zones. Due to heat island circulation, the urban humidification effect is more pronounced (Han et al. 2014). However, cities in the YRD show significant states of "warm and dry" ($\triangle T > 0$ and $\triangle RH < 0$ in Fig. 7a–f), and the promotion effect of the UHI on urban HR is stronger than the inhibition effect of the UDI on urban HR (α_{YRD} in Fig. 7a, c > α_{YRD} in Fig. 7b, d, respectively). In addition, due to the strong negative correlation between $\triangle T$ and $\triangle RH$ in the YRD (the correlation coefficient is − 0.88 and passed the 99% significance test), the UDI shows a negative effect on HR in the afternoon (12:00–18:00) (Fig. 7d), which means that the combined impacts of the UHI and UDI on HR may be nonlinear. For the MUYR, NCP, and NEC, HR is more sensitive to humidity, especially in the afternoon (12:00–18:00), indicating that the UDI has a greater inhibitory effect on HR than the promotion effect of the UHI on HR (α_{MUYR}, α_{NCP}, and α_{NEC} in Fig. 7c > α_{MUYR}, α_{NCP}, and α_{NEC} in Fig. 7d, respectively). Generally, UDI results in reductions in urban HR by lowering the conversion efficiency to precipitation when water vapor is insufficient. In the MUYR and NCP (where $\triangle T > 0$ and $\triangle RH < 0$ in Fig. 7a–f), HR is greatly suppressed by humidity shortages, which means that a greater UDI intensity corresponds to lower urban HR (Fig. 7b, d). However, the negative HR differences between urban and rural areas in NEC mostly occur in the afternoon (12:00–18:00) (Fig. 7a–d), where the inhibitory effect of the UDI on HR is the strongest in the five climate regions (α_{NEC} in Fig. 7d > α_{NEC} in Fig. 7c). The differences between the YRD and NCP were partially confirmed by Zhao et al. (2019), whose study supported that Q_1 (atmospheric heat source, which reflects local heat sources) in the YRD was greater than that in the NCP, which is more obvious during the daytime. Q_2 (water vapor sink, reflecting local

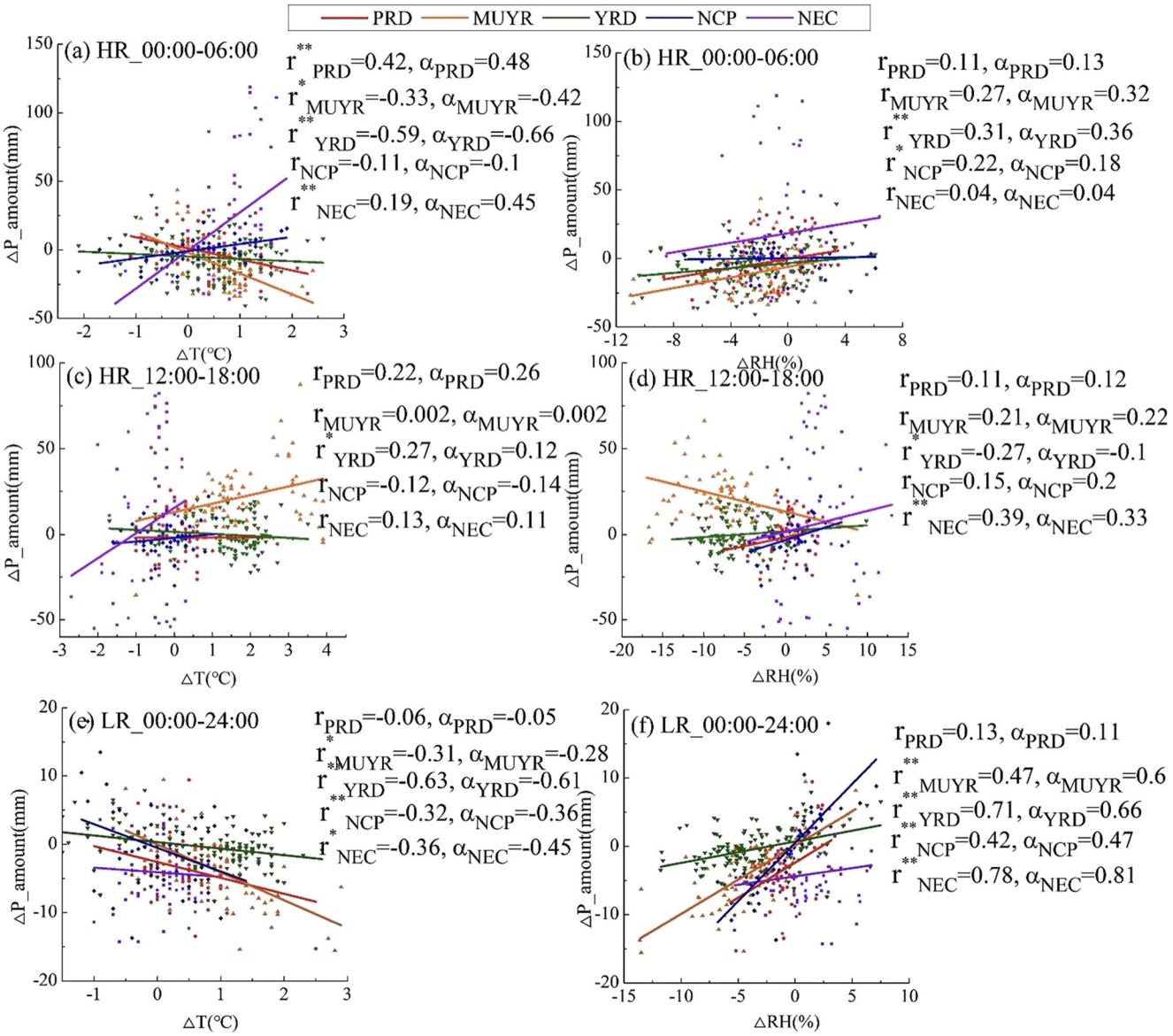

Fig. 7 Relationship between urban-rural precipitation differences and the UHI and UDI in various regions. The relationship between **a** HR urban-rural differences from 00:00 to 06:00 and UHI at 02:00, **b** HR urban-rural differences from 00:00 to 06:00 and UDI at 02:00, **c** HR urban-rural differences from 12:00 to 18:00 and UHI at 14:00, **d** HR urban-rural differences from 12:00 to 18:00 and UDI at 14:00, **e** LR urban-rural differences for all day and diurnal average UDI, and **f** LR urban-rural differences for all day and diurnal average UHI. *r* represents the fitting coefficient, α is the normalized slope, ** indicates that the value passed the 99% significance test, and * indicates that the value passed the 98% significance test

evaporation conditions) in the YRD was larger than that in the NCP, which was more obvious at night. Their results showed that the intensity of the UHI in the YRD was greater than that in the NCP during the daytime and less than that in the NCP at night, which indicated that the YRD has more thermal energy than the NCP and more water vapor and a stronger UHI effect during the daytime. Therefore, the YRD is more prone to convective movement during the daytime, and the strong UHI effect will further promote the occurrences of urban HR. However, the NCP has less thermal energy and water vapor and shows weak convective movement and UHI effects during the daytime; moreover, urban HR is weakly promoted by the UHI and may mainly suppressed by the UDI.

LR is mainly inhibited by the UDI in the five climate regions, which resulted in more LR over rural areas than urban areas. The combined effects of the UHI and UDI make the urban areas drier, which increases the likelihood of small raindrops evaporating in urban areas. On the other hand, the higher temperature of the urban boundary layer increases the height of the urban water vapor condensation layer and zero-degree layer as well as the cloud

base height and the raindrop path, ultimately increasing the possibility of small raindrop evaporation (Kaufmann et al. 2007). As △T becomes large, the corresponding △RH becomes small (negative value), and both effects lead to less LR in urban areas than rural areas (Fig. 7e–f). The effect of the UDI on LR is higher than that of the UHI in all regions (α in Fig. 7f > α in Fig. 7e), indicating that LR is still mainly suppressed by UDI.

4 Conclusions

This study uses a 30-year (1983–2012) summer meteorological observational data and ECMWF reanalysis data to reveal the precipitation differences between urban and rural areas. The precipitation is divided into two categories based on intensity (HR and LR), and the study regions include five different climate regions (PRD, MUYR, YRD, NCP, and NEC) in central and eastern China. The relative dependence of precipitation on meteorological factors (UHI, UDI, CAPE, water vapor content in the whole atmospheric layer, and dew-point deficit) is analyzed, which explains the inconsistent urbanization effects on precipitation over different typical climate regions. The main conclusions are as follows:

(1) Urbanization shows inconsistent effects on precipitation at different intensities and in different climate regions. LR is greater over rural areas than urban areas. HR is higher over the urban areas of the PRD and YRD than rural areas, while HR is lower over the urban areas of the MUYR, NCP and NEC than rural areas. This phenomenon is similar to trends found for the precipitation amounts, precipitation counts, and precipitation durations.

(2) There are no obvious differences between urban and rural areas in precipitation diurnal variations, although the afternoon peak of HR in urban areas is slightly earlier than that in rural areas, which may be related to the ability of the UHI to trigger precipitation formation conditions faster.

(3) The inconsistent effects of urbanization on HR in different climate regions can be explained by the relative dependence of precipitation on the CAPE and humidity in various climate regions. The HR is greatly affected by the CAPE in the PRD and YRD (β_{PRD} = 0.44 and β_{YRD} = 0.35 in Fig. 6b > β_{PRD} = 0.29 and β_{YRD} = 0.16 in Fig. 6a), where convective movements are strong and water vapors are abundant (CAPE > 600 J/kg at 14:00 LT and water vapor content > 45 kg/m^2 at 14:00 LT). Therefore, higher HR occurs in urban areas because of the UHI. In contrast, the HR is greatly affected by humidity in the MUYR, NCP, and NEC (β_{MUYR} = 0.28, β_{NCP} = 0.41, β_{NEC} = 0.5 in Fig. 6a > β_{MUYR} = 0.08, β_{NCP} = 0.19, β_{NEC} = 0.42 in Fig. 6b), where the water vapor contents and convective instability energy are less (CAPE ≤ 500 J/kg and water vapor content ≤ 40 kg/m^2 at 14:00 LT) and the UDI impacts suppress HR in urban areas. Finally, the LR has a good correlation with humidity in all regions, which means that LR is mainly affected by the suppression impacts of the UDI and less LR is seen in urban areas than rural areas.

The results of this study indicate that urbanization promotes HR in wet climates (PRD and YRD), suppresses HR in dry climates (MUYR, NCP, and NEC), and suppresses LR in all regions of central and eastern China during summer. Since the physical mechanisms underlying the above conclusions are based on statistical analyses and the results of other researchers' literature, a deeper investigation needs to be carried out with the help of future model analyses.

Funding This work is supported by the National Key Research and Development Program of China (2016YFA0602003) and the National Natural Science Foundation of China (Grant No. 41575148).

References

Baik JJ (1992) Response of a stably stratified atmosphere to low-level heating an application to the heat island problem. J Appl Meteorol 31:291–303

Baik JJ, Kim YH, Chun HY (2001) Dry and moist convection forced by an urban heat island. J Appl Meteorol 40:1462–1475

Baik JJ, Kim YH, Kim JJ et al (2007) Effects of boundary-layer stability on urban heat island-induced circulation. Theor Appl Climatol 89: 73–81

Bornstein R, Lin Q (2000) Urban heat islands and summertime convective thunderstorms in Atlanta: three case studies. Atmos Environ 34: 507–516

Changnon SA (1979) Rainfall changes in summer caused by St. Louis. Science 205:402–404

Choi YS, Ho CH, Kim J, Gong DY, Park RJ (2008) The impacts of aerosols on the summer rainfall frequency in China. J Appl Meteorol Climatol 47:1802–1813

Dong WH, Lin YL, Wright JS, Xie Y, Yin X, Guo J (2019) Precipitable water and CAPE dependence of rainfall intensities in China. Clim Dyn 52:3357–3368

Guo JX (2014) Research on environmental standards for surface meteorological elements observation (in Chinese). China Sci Technol Achiev 15:30–32

Guo X, Fu D et al (2014) A case study of aerosol impacts on summer convective clouds and precipitation over northern China. Atmos Res 142:142–157

Guo J, Li GP (2009) Climatic characteristics of precipitable water vapor and relations to surface water vapor column in Sichuan and Chongqing Region (in Chinese). J Nat Resour 24:344–350

Guo T, Zhu B, Kang Z, Gui H, Kang H (2016) Spatial and temporal distribution characteristic of fog days and haze days from 1960–2012 and impact factors over the Yangtze River Delta Region (in Chinese). China Environ Sci 36:961–969

Han JY, Baik JJ (2008) A theoretical and numerical study of urban heat island-induced circulation and convection. J Atmos Sci 65:1859–1877

Han JY, Baik JJ, Lee H (2014) Urban impacts on precipitation. Asia-Pac J Atmos Sci 50:17–30

Hao Z, Aghakouchak A, Phillips TJ (2013) Changes in concurrent monthly precipitation and temperature extremes. Environ Res Lett 8:1402–1416

He LQ, Yang P, Jing X et al (2017) Analysis of temporal-spatial variation of heat island effect in Pearl River Delta using MODIS images and impermeable surface area. Remote Sens Land Resour 29:140–146

Houze RA (1993) Cloud Dynamics. Academic Press, New York

Hua L, Ma Z, Guo W (2008) The impact of urbanization on air temperature across China. Theor Appl Climatol 93:179–194

Jiang JX, Fan MZ (2002) Convective clouds and mesoscale convective systems over the Tibetan Plateau in summer (in Chinese). Chin J Atmos Sci 26:263–270

Jiang ZH, Li Y, Huang DL (2016) Impact of urbanization in different regions of eastern china on precipitation and its uncertainty. J Trop Meteorol 461:382–392

Jiao MY, Li C, Li YX (2005) Mesoscale analyses of a Sichuan heavy rainfall (in Chinese). J Appl Meteor Sci 16:699–704

Kaufmann RK, Seto KC, Schneider A, Liu Z, Zhou L, Wang W (2007) Climate response to rapid urban growth: evidence of a human-induced precipitation deficit. J Clim 20:2299–2306

Kishtawal CM, Niyogi D, Tewari M et al (2010) Urbanization signature in the observed heavy rainfall climatology over India. Int J Climatol 30:1908–1916

Lepore C, Veneziano D, Molini A (2015) Temperature and CAPE dependence of rainfall extremes in the eastern United States. Geophys Res Lett 42:74–83

Li WB, Chen S, Chen GX, Sha W, Luo C, Feng Y, Wen Z, Wang B (2011a) Urbanization signatures in strong versus weak precipitation over the Pearl River Delta metropolitan regions of China. Environ Res Lett 6:034020

Li XX, Koh TY, Panda J et al (2016) Impact of urbanization patterns on the local climate of a tropical city, Singapore: an ensemble study. J Geophys Res Atmos 121:4386–4403

Li ZQ, Niu F, Fan JW et al (2011b) Long-term impacts of aerosols on the vertical development of clouds and precipitation. Nat Geosci 4:888–894

Li ZQ, Wang Y, Guo JP, Zhao CF, Cribb MC, Dong XQ et al (2019) East Asian study of tropospheric aerosols and their impact on regional clouds, precipitation, and climate (EAST-AIR$_{CPC}$). J Geophys Res Atmos 124:13026–13054

Liang P, Ding YH (2017) The long-term variation of extreme heavy precipitation and its link to urbanization effects in Shanghai during 1916–2014. Adv Atmos Sci 34:321–334

Liang L, Li YQ, Hu HR et al (2013) Numerical simulation of the relationship between summer susceptibility anomalies on the Qinghai-Tibet Plateau and precipitation in Sichuan and Chongqing areas (in Chinese). Plateau Meteorol 32:1538–1545

Lin CY, Chen WC, Chang PL, Sheng YF (2011) Impact of the urban heat island effect on precipitation over a complex geographic environment in Northern Taiwan. J Appl Meteorol Climatol 50:339–353

Miao S, Chen F, Li Q, Fan S (2011) Impacts of urban processes and urbanization on summer precipitation: a case study of heavy rainfall in Beijing on 1 August 2006. J Appl Meteorol Climatol 50:806–825

Mote TL, Lacke MC, Shepherd JM (2007) Radar signatures of the urban effect on precipitation distribution: a case study for Atlanta, Georgia. Geophys Res Lett 34:20710

Ntelekos AA, Donner L, Fast JD, Gustafson WI, Chapman EG, Krajewski WF (2009) The effects of aerosols on intense convective precipitation in the northeastern United States. Quart J Roy Meteor Soc 135:1367–1391

Oke TR (1973) City size and the urban heat island. Atmos Environ 7: 769–779

Olfe DB, Lee RL (1971) Linearized calculations of urban heat island convection effects. J Atmos Sci 28:1374–1388

Pruppacher HR, Klett JD (1997) Microphysics of clouds and precipitation. Kluwer Academic Publishers, Netherlands

Rosenfeld D (1999) TRMM observed first direct evidence of smoke from forest fires inhibiting rainfall. Geophys Res Lett 26:3105–3108

Rosenfeld D (2000) Suppression of rain and snow by urban and industrial air pollution. Science 287:1793–1796

Rosenfeld D, Lohmann U, Raga GB, O'Dowd CD, Kulmala M, Fuzzi S, Reissell A, Andreae MO (2008) Flood or drought: how do aerosols affect precipitation? Science 321:1309–1313

Rozoff CM, Cotton WR, Adegoke JO (2003) Simulation of St. Louis, Missouri, land use impact on thunderstorms. J Appl Meteorol 42: 716–738

Shastri H, Paul S, Ghosh S, Karmakar S (2015) Impacts of urbanization on Indian summer monsoon rainfall extremes. J Geophys Res Atmos 120:495–516

Shem W, Shepherd M (2009) On the impact of urbanization on summertime thunderstorms in Atlanta: two numerical model case studies. Atmos Res 92:172–189

Song X, Zhang J, Aghakouchak A et al (2014) Rapid urbanization and changes in spatiotemporal characteristics of precipitation in Beijing metropolitan area. J Geophys Res Atmos 119:11250–11271

Souma K, Tanaka K, Suetsugi T, Sunada K, Tsuboki K, Shinoda T, Wang Y, Sakakibara A, Hasegawa K, Moteki Q, Nakakita E (2013) A comparison between the effects of artificial land cover and anthropogenic heat on a localized heavy rain event in 2008 in Zoshigaya, Tokyo, Japan. J Geophys Res Atmos 118:11600–11610

Tayan M, Toros H (1997) Urbanization effects on regional climate change in the case of four large cities of Turkey. Clim Chang 35: 501–524

Wang J, Feng J, Yan Z (2015) Potential sensitivity of warm season precipitation to urbanization extents: modeling study in Beijing-Tianjin-Hebei urban agglomeration in China. J Geophys Res Atmos 120:9408–9425

Wu FB, Tang JP (2015) Impact of urbanization on summer precipitation and temperature in the Yangtze River Delta (in Chinese). J Trop Meteorol 31:255–263

Yan SQ, Zhu B, Kang HQ (2019) Long-term fog variation and its impact factors over polluted regions of East China. J Geophys Res Atmos 124:1741–1754

Yang G, Bowling LC, Cherkauer KA, Pijanowski BC (2011) The impact of urban development on hydrologic regime from catchment to basin scales. Landsc Urban Plan 103:237–247

Yang Y, Wu B, Shi C, Zhang J, Li Y, Tang W, Shi T (2013) Impacts of urbanization and station-relocation on surface air temperature series in Anhui Province, China. Pure Appl Geophys 170:1969–1983

Zhang CL, Chen F, Miao SG et al (2009) Impacts of urban expansion and future green planting on summer precipitation in the Beijing metropolitan area. J Geophys Res Atmos 114:356–360

Zhang N, Gao Z, Wang X et al (2010) Modeling the impact of urbanization on the local and regional climate in Yangtze River Delta, China. Theor Appl Climatol 102:331–342

Zhao XT, Zhu B, Pan C (2019) Research on temperature difference of urban-rural areas in different climate in central-eastern China (in Chinese). J Meteorol Sci 39:569–577

Zhou L, Jiang ZH, Li ZX et al (2015) Simulation of climate effects of underlying surface changes in different urban agglomerations in eastern China (in Chinese). Chin J Atmos Sci 39:596–610